



OPEN

Fast cooling in dispersively and dissipatively coupled optomechanics

SUBJECT AREAS:

NEMS

THEORETICAL PHYSICS

Tian Chen^{1,2} & Xiang-Bin Wang^{1,2,3}

¹State Key Laboratory of Low Dimensional Quantum Physics, Department of Physics, Tsinghua University, Beijing 100084, People's Republic of China, ²Synergetic Innovation Center of Quantum Information and Quantum Physics, University of Science and Technology of China, Hefei, Anhui 230026, People's Republic of China, ³Jinan Institute of Quantum Technology, Shandong Academy of Information and Communication Technology, Jinan 250101, People's Republic of China.

Received
18 July 2014Accepted
1 December 2014Published
13 January 2015

Correspondence and
requests for materials
should be addressed to
X.-B.W. (xbwang@
mail.tsinghua.edu.cn)

The cooling performance of an optomechanical system comprising both dispersive and dissipative coupling is studied. Here, we present a scheme to cool a mechanical resonator to its ground state in *finite time* using a chirped pulse. We show that there is distinct advantage in using the chirp-pulse scheme to cool a resonator rapidly. The cooling behaviors of dispersively and dissipatively coupled system is also explored with different types of incident pulses and different coupling strengths. Our scheme is feasible in cooling the resonator for a wide range of the parameter region.

Cool a mechanical resonator to its ground state is of fundamental importance in many quantum information processing and metrological experiments: ultrahigh sensitive detection, the observation of quantum behavior in a mechanical oscillator, and so forth. The subject has therefore attracted much attention from researchers in recent years^{1,2}. In many of these schemes, an auxiliary system is introduced to cool the mechanical resonator. The ground state cooling of a mechanical resonator is realized by coupling the resonator with a driven cavity via radiation pressure (a dispersively coupled optomechanics)³, e.g. backaction cooling via a detuning cavity, cold-damping quantum feedback cooling⁴⁻⁷, and other methods⁸⁻¹⁶. By employing a chirped pulse, the phonon occupation of the mechanical resonator is reduced to a very small value quickly¹¹⁻¹³. Experimental realization of cooling scheme for a mechanical resonator has been implemented¹⁷⁻²⁶. By combining sideband cooling technique with cryogenic cooling, the position of the cooled resonator has been measured^{20,21}. Recently, a quantum coherent exchange between the mechanical system and the micro/optical wave is achieved^{25,26}, and the phonon occupation number of the cooled resonator is reduced to single-phonon level.

In several recent microwave optomechanical experiments²⁷⁻³², it is shown that dissipative coupling, in which the cavity damping strength is modulated by the motion of mechanical resonator, should be considered for the cooling of resonator, aside from dispersive coupling. Theoretical studies also show that the coexistence of the dispersive coupling and dissipative coupling leads to the phenomenon of the quantum destructive interference in the mechanical resonator cooling³³⁻³⁶. In such a dispersively and dissipatively coupled system, the optimal cavity driven frequency depends significantly on the ratio of the dispersive coupling strength to the dissipative coupling strength. Moreover, in the microdisk-waveguide optomechanical system experiment³⁷, it has been demonstrated that the force from the dissipative coupling dominates the total force applied to the waveguide in such dispersively and dissipatively coupled system.

In this paper, we study the rapid cooling of mechanical resonator for systems that are subject to both dispersive and dissipative coupling. With a chirped pulse, the fast cooling of a mechanical resonator can be realized within a short time. We show that, by modulating the incident pulses, the phonon occupation of the resonator can be reduced to single-phonon level. When the chirped pulse is applied in a pure dissipatively coupled optomechanical system, the cooling performance of the resonator becomes better with increasing cavity damping strength. In comparison, this is different from the optomechanical system that possesses only dispersive coupling, where it is shown that the cooling of the mechanical resonator improves with a smaller cavity damping strength, as shown by Liao and Law¹³. We also explore the cooling performance of our scheme with different frequency-sweep strengths. Moreover, we show that our scheme is effective for a wide range of dispersive and dissipative coupling strengths.



Results

The description of the system and its solution. We consider an optomechanical system consisting of a mechanical resonator and a cavity mode. Taking into account both dispersive and dissipative coupling, the system is described by the Hamiltonian³³,

$$H = \omega_c a^\dagger a + \omega_m b^\dagger b + H_\kappa + H_\gamma - \left(A \kappa a^\dagger a + i \sqrt{\frac{\kappa}{2\pi\rho}} \frac{B}{2} \sum_q (a^\dagger b_q - b_q^\dagger a) \right) (b^\dagger + b). \quad (1)$$

Here, we have used the following notations: ω_c is the cavity frequency, ω_m is the resonance frequency of the mechanical oscillator, a (a^\dagger) is the annihilation (creation) operator of the cavity mode, b (b^\dagger) is the annihilation (creation) operator of the mechanical resonator, H_κ and H_γ are the damping of the cavity and mechanical resonator, respectively, A (B) is the dispersive (dissipative) coupling strength, κ is the cavity damping strength, b_q (b_q^\dagger) is the annihilation (creation) operator of the optical bath coupled to the cavity mode, and ρ is the density of state for the optical bath. Using the Heisenberg equation, we obtain^{36,38},

$$\sqrt{\frac{\kappa}{2\pi\rho}} \sum_q b_q = \sqrt{\kappa} a_{in} + \frac{\kappa}{2} a + \frac{\kappa B}{2} (b + b^\dagger) a, \quad (2)$$

the input-output relation is

$$a_{out} - a_{in} = \sqrt{\kappa} a + \frac{\kappa}{2} a + \frac{\kappa B}{2} (b + b^\dagger) a, \quad (3)$$

where a_{in} is the input mode. The Hamiltonian is linearized and each operator is separated into a mean amplitude and a fluctuation component. Using $a = (\langle a \rangle + \delta a) e^{-i\omega_d t}$, $b = \langle b \rangle + \delta b$, and $a_{in} = (\langle a_{in} \rangle + \xi_{in}) e^{-i\omega_d t}$, ω_d is the frequency of the driven field, ξ_{in} is the noise induced by the optical bath. The detailed expressions of dynamics of the fluctuation components δa , δb as well as the mean amplitudes $\langle a \rangle$, $\langle b \rangle$, are described in Methods section.

Our aim is to reduce the value of fluctuation components $\langle \delta b^\dagger \delta b \rangle$. A covariance matrix notation $R_{l,l'}(t) = \langle v_l(t) v_{l'}(t') \rangle$ is introduced. v_l is the l th element of \vec{V} , the vector \vec{V} is constructed from such four fluctuation components,

$$\vec{V}(t) = [\delta a, \delta b, \delta a^\dagger, \delta b^\dagger]^T. \quad (4)$$

The dynamics of R is formulated as

$$R(t) = G(t)R(0)G(t)^T + G(t)Z(t)G(t)^T. \quad (5)$$

The explicit forms of the above parameters, i.e. $G(t)$, $Z(t)$, are given in details in the Methods section. We assume that the initial optical bath is a zero-temperature bath, the initial condition $R(0)$ has three nonzero elements, $R_{13}(0) = 1$, $R_{24}(0) = N_{th} + 1$, and $R_{42}(0) = N_{th}$. Based on the definition of the covariance matrix $R_{l,l'}(t)$, we then obtain the time-dependent mean displaced phonon number as $\langle \delta b^\dagger \delta b \rangle = R_{42}(t)$, and the mean displaced photon number $\langle \delta a^\dagger \delta a \rangle = R_{31}(t)$.

Cooling of the resonator with chirped pulse. Chirped pulse form.

The chirped pulse has been employed to convert the population of a two-level-system efficiently^{11,12}. In our dispersively and dissipatively coupled optomechanics, the interaction between the cavity mode and the mechanical resonator mode (δa and δb) has a form similar to the optical-matter interaction^{11–13}. The incident chirped pulse is designed as follows: $A \kappa \langle a(t) \rangle - \Omega(t) \frac{B}{2} = \chi(t) \cdot e^{i\phi(t)}$, $\chi(t) = \chi_0 \cdot \text{sech}(\alpha(t - t_0))$, the frequency sweep $\phi(t) = \beta \tanh(\alpha(t - t_0))$, the amplitude of the coherent laser drive $\Omega(t)$ as shown in Methods section. We present the performance of such a chirped pulse in the

cooling of mechanical resonator below for our optomechanical system with two couplings.

We numerically obtain the residual phonon number of the mechanical resonator ($\langle \delta b^\dagger \delta b \rangle$) as a function of time. For comparison, two different schemes are provided: with chirped pulse (chirped pulse scheme) and without the chirped pulse (no-chirped pulse scheme). The different driven frequencies ω_d are discussed below. Here, the cavity detuning is $\Delta = \omega_d - \omega_c$. From Fig. 1(a), when $\Delta/\omega_m = -1$, we find that at time $\omega_m t = 80$ or longer, the phonon number of the mechanical resonator can be reduced to a relatively low value and kept stable for the chirped pulse cooling scheme. The figure inset shows the amplitude of the laser drive $\Omega(t)$ with time. By employing the Fourier transform, we find that the full width at half maximum (FWHM) of such a pulse $\Omega(t)$ is about $0.05\omega_m$. So for the case of $\omega_m t_0 = 40$, the effect of pulse bandwidth is neglectable. While, for the no-chirped pulse scheme, the cooling effect of the resonator is not well-behaved, and the phonon number changes with time drastically. Although the small phonon occupation number of the resonator is achieved in the no-chirped pulse case for some time interval, the phonon occupation quickly raises to a high value at later time. It means that we do not achieve perfect cooling of resonator with the no-chirped pulse scheme. Next, another driven frequency is applied ($\Delta/\omega_m = 0.5$). In our parameters settings ($A = 0$, $B \neq 0$, a purely dissipative optomechanics), this value of driven frequency is the optimal one for the steady state cooling of resonator^{33,35,36}. The cooling behaviors with different cavity damping strengths are shown in Fig. 1(b) and (c). Compared with the cooling results of the no-chirped pulse scheme, an improved cooling performance of the resonator is achieved with the chirped pulse. Taking the cavity damping strength $\kappa/\omega_m = 0.5$ as an example, in the chirped pulse scheme, at time $\omega_m t = 70$, the mechanical resonator number ($\langle \delta b^\dagger \delta b \rangle$) reaches the value 1.6, which is much smaller than the case with the no-chirped pulse scheme.

We explore the relation between the cooling of resonator ($\langle n_{osc} \rangle$) and the cavity damping strength (κ) for the chirped pulse scheme. Fig. 2(a) and Fig. 2(b) illustrate the situation when the cavity driven frequency satisfies $\Delta/\omega_m = 0.5$. When the cavity damping strength increases, we achieve a smaller phonon occupation of the resonator. From Eq. 7 in Methods section, we show that the time evolution of cavity mode operator δa is affected by the intrinsic damping term $F_1(t)$, the interaction term $F_2(t)$ associated with the mechanical mode δb , and the noise induced from the optical bath $F_3(t)$. The detailed expression of $F_1(t)$, $F_2(t)$, and $F_3(t)$ is given by Eq. 11, 12, 13 in Methods section. From Fig. 2(b), we find that the value of $|F_1(t)|$, $|F_2(t)|$ and $|F_3(t)|$ rise with the increase of the cavity damping strength κ . This means that the damping of cavity mode δa and interaction between the cavity mode δa and the mechanical resonator mode δb both increase. The energy of the resonator is quickly transferred to the zero-temperature cavity mode, and then is dissipated into the bath rapidly. This is why we can obtain the smaller phonon occupation of the resonator with the larger cavity damping strength.

Moreover, we study the relation between the cavity damping strength (κ) and the steady-state phonon number of the mechanical resonator in the no-chirped pulse scheme. Our aim is to reveal the different cooling behaviors between the purely dispersively and purely dissipatively coupled optomechanics, when the cavity driven frequency is chosen optimal in steady-state cooling. For the no-chirped pulse scheme, the mechanical intrinsic damping (Σ_{eq}) and quantum backaction force from the driven cavity (S_{bac}) contribute to the final phonon occupation of resonator at steady-state

$$\langle n_{osc} \rangle = \int \frac{d\omega}{2\pi} S_{cc}(\omega) = \Sigma_{eq} + S_{bac} = \int \frac{d\omega}{2\pi} \frac{\gamma \sigma_{th}(\omega)}{|N(\omega)|^2} + \int \frac{d\omega}{2\pi} \frac{\kappa \sigma_{opt}(\omega)}{|N(\omega)|^2}, \quad (6)$$

where $S_{cc}(\omega)$ is the mechanical spectrum, $\sigma_{th}(\omega)$ is a quantity related to the mechanical thermal bath and optomechanical self-energy, $\sigma_{opt}(\omega)$ combines the intracavity amplitude and quantum backaction

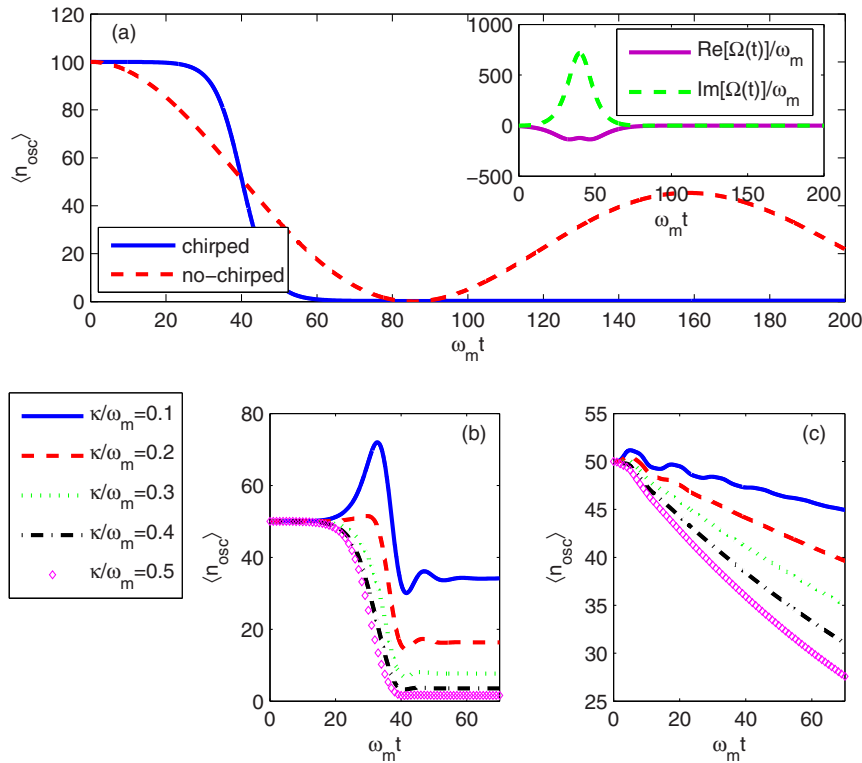


Figure 1 | The time evolution of the phonon number $\langle n_{osc} \rangle = \langle \delta b^\dagger \delta b \rangle$. (a) Blue solid one denotes the chirped pulse form, red dashed one is the no-chirped form. Other parameters: $A = 0$, $B = 2 * 10^{-4}$, $\kappa/\omega_m = 0.01$, $\gamma/\omega_m = 10^{-5}$, $N_{th} = 100$, $\langle a(0) \rangle = 200$, $\Delta/\omega_m = -1$. For the chirped pulse form, $\alpha/\omega_m = 0.14$, $\beta/\omega_m = 0.04$, $\chi_0 = \frac{1}{2} \sqrt{\alpha^2 + \beta^2}$, $\omega_m t_0 = 40$. (b) (chirped pulse form) and (c) (no-chirped pulse form), $A = 0$, $B = 2 * 10^{-4}$, $\gamma/\omega_m = 10^{-6}$, $N_{th} = 50$, $\langle a(0) \rangle = 10^3$, $\Delta/\omega_m = 0.5$; for the chirped pulse form (b), $\alpha/\omega_m = 0.15$, $\beta/\omega_m = 0.05$, $\chi_0 = \frac{3}{2} \sqrt{\alpha^2 + \beta^2}$, $\omega_m t_0 = 30$.

force spectrum. $N(\omega)$ comprises the response function of the mechanical resonator and optomechanical self-energy. κ and γ are the cavity damping strength and mechanical intrinsic damping strength, respectively. The pure dispersive coupling case is shown in Fig. 3(a), and the cavity driven frequency is optimal, $\Delta/\omega_m = -1$. In such a case, the phonon occupation of resonator decreases with cavity damping strength κ first, then rises up quickly. Fig. 3(b) and (c) show the pure dissipative coupling case with cavity detunings $\Delta/\omega_m = -1$ and $\Delta/\omega_m = 0.5$, respectively. When the cavity detuning is optimal ($\Delta/\omega_m = 0.5$, see Fig. 3(c)), the residual phonon number of the resonator decreases with an increase in the cavity damping strength. It is noted that, for such a dissipatively coupled system, the relation between the residual phonon number of the steady-state cooling and the cavity damping strength is similar to the relation for the chirped pulse cooling as shown in Fig. 2(a).

Next, we show the advantage of the chirped pulse scheme explicitly. We compare the cooling behaviors of the mechanical resonator with and without chirped pulses. When considering such a purely dissipatively coupled optomechanics, we allow the cavity driven frequency in the no-chirped pulse scheme to satisfy $\Delta/\omega_m = 0.5$. At such an optimal detuning, the cavity acts as an effective zero-temperature bath³³. From Fig. 4, we find that by employing the chirped pulse, the mean resonator number is reduced to less than one quickly and kept such a low population for a long time. We need to mention that, the rise of the phonon number of the resonator after the pulse duration is due mainly to the heating from the bath of mechanical resonator¹³. In our discussion, the phonon number increases from 0.14 to 1.08 with the time varying from $\omega_m t = 80$ to $\omega_m t = 2000$. Considering the fact that the initial phonon occupation of the resonator is $N_{th} = 50$, such a rise of phonon number from 0.14 to 1.08 after the pulse duration is actually rather small. In contrast, for the no-chirped pulse scheme, we do not even achieve the ground state of resonator at time $\omega_m t = 2000$. So, the chirped pulse scheme provides

a new way to cool the resonator in *finite time* duration, and this is helpful for controlling the state of the resonator.

We now discuss the universality of the chirped pulse scheme in resonator cooling. The evolution time is $\omega_m t = 70 \geq 2t_0$. Firstly, the effect of the different strengths of frequency sweeping field and optomechanical coupling strength ratios (dispersive coupling strength/dissipative coupling strength) is shown in Fig. 5(a). In the region of $0.08 \leq |\beta/\omega_m| \leq 0.18$, the mean residual occupation is lower than one. This result is insensitive to the strength of sweeping field. It is well known that the dispersive coupling and dissipative coupling strength can be modulated in the designed scheme^{30,31}. So we can achieve the ground state cooling of the mechanical resonator with different dispersive and dissipative coupling strengths. Secondly, we explore the effects of the cavity detunings. The residual phonon number of the mechanical resonator with the chirped pulse scheme and no-chirped pulse scheme are compared in Fig. 5(b) and (c). For the chirped pulse case (b), we can reduce the phonon occupation of the resonator to one in the vicinity of $\Delta/\omega_m = -1$, with the coupling strength ratio $A/B \leq 0.2$. The resonator is cooled to around one phonon with the coupling strength ratio $A/B \geq 5$ in the no-chirped pulse scheme (c). When we choose the ratio $A/B \geq 5$ and $\Delta/\omega_m \approx -1$ in the chirped pulse case, the mean phonon occupation of the resonator is smaller than three. Although it might not be easy to achieve the same effective cooling performance as the no-chirped pulse scheme in the region $A/B \geq 5$, the chirped pulse scheme can cool the resonator efficiently for a much wider region, $5 * 10^{-3} \leq A/B \leq 10$. Finally, in the pure dissipative coupling case, the influence of the frequency sweep and cavity detuning on the phonon occupation is shown in Fig. 5(d) and (e). A better cooling effect appears when the frequency sweep value $|\beta/\omega_m|$ is relatively large. In the region around $\Delta/\omega_m = -1$ and $\Delta/\omega_m = 0.4$, we reduce the residual phonon occupation of the resonator below one when the strength of sweeping field is chosen as $\beta/\omega_m = 0.125$.

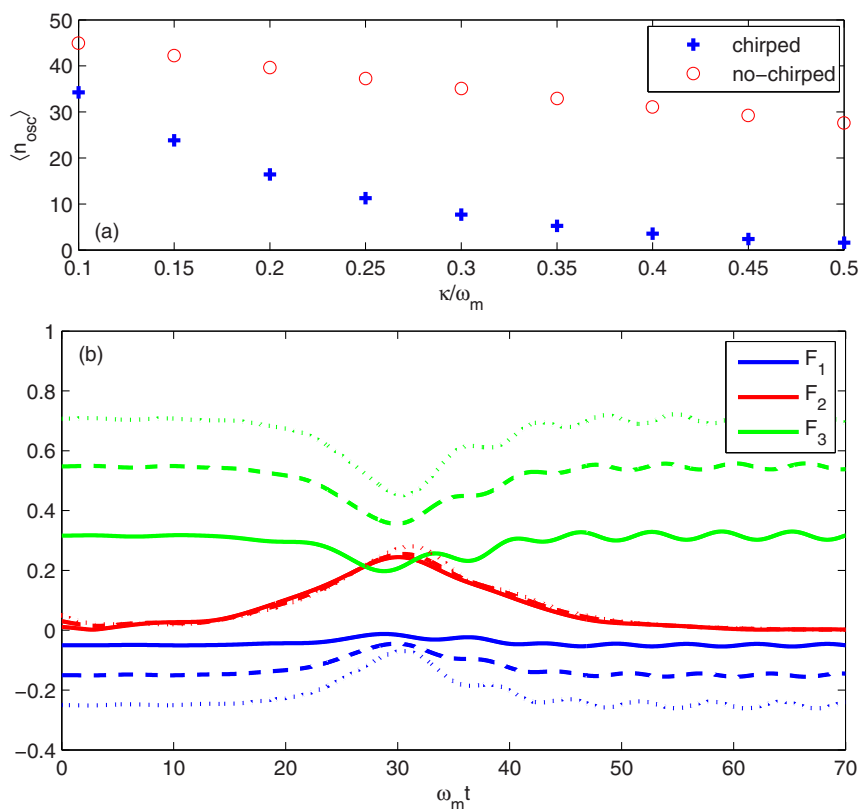


Figure 2 | (a), the residual phonon number $\langle n_{osc} \rangle = \langle \delta b^\dagger \delta b \rangle$ at time $\omega_m t = 70$, with the increase of cavity damping strength. Parameters set, $\Delta/\omega_m = 0.5$, $A = 0$, $B = 2 * 10^{-4}$, $\gamma/\omega_m = 10^{-6}$, $N_{th} = 50$, $\langle a(0) \rangle = 10^3$. For the chirped pulse form (blue cross term), $\alpha/\omega_m = 0.15$, $\beta/\omega_m = 0.05$, $\chi_0 = \frac{3}{2} \sqrt{\alpha^2 + \beta^2}$, $\omega_m t_0 = 30$, the amplitude of F_1 , F_2 , and F_3 with time evolution. Solid, $\kappa/\omega_m = 0.1$; dashed, $\kappa/\omega_m = 0.3$; dotted, $\kappa/\omega_m = 0.5$. Other parameters are same as in (a).

Discussion and conclusion

In summary, we have extensively studied the cooling of a mechanical resonator for the system consisting of *both* dispersive coupling and

dissipative coupling in *finite time*. As stated in Ref. 13, the authors employ a chirped pulse to cool the mechanical resonator efficiently in a dispersively coupled optomechanics. The pulse shape is found in

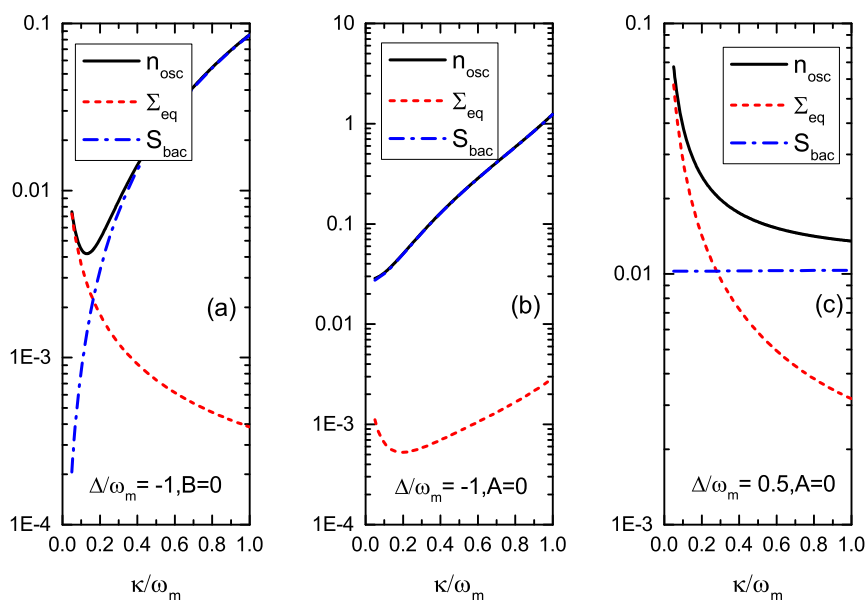


Figure 3 | The steady-state phonon number $\langle n_{osc} \rangle = \langle \delta b^\dagger \delta b \rangle$, the intrinsic oscillator damping Σ_{eq} , the backaction from the cavity S_{bac} with the cavity damping strength κ : (a), pure dispersive coupling case, $A = 2 * 10^{-4}$, $B = 0$, $\Delta/\omega_m = -1$; (b), pure dissipative coupling case, $A = 0$, $B = 2 * 10^{-4}$, $\Delta/\omega_m = -1$; (c), pure dissipative coupling case, $A = 0$, $B = 2 * 10^{-4}$, $\Delta/\omega_m = 0.5$. For all of three plots, $\gamma/\omega_m = 10^{-6}$, $N_{th} = 50$, intra-cavity amplitude at the steady state, $\langle a \rangle = 10^3$.

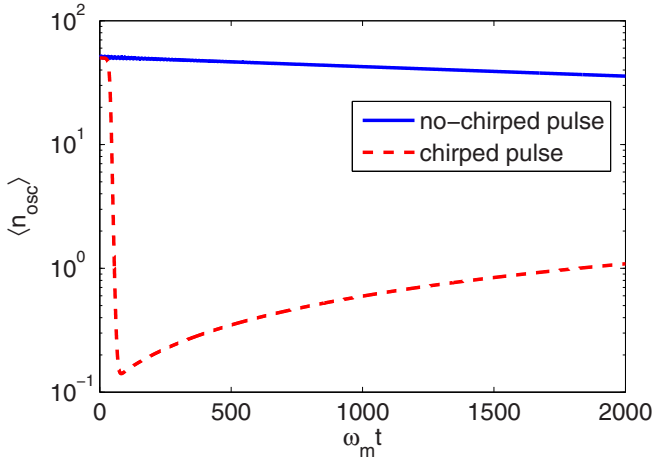


Figure 4 | The time evolution of the phonon number $\langle n_{osc} \rangle = \langle \delta b^\dagger \delta b \rangle$. Red dashed, the chirped pulse form, $\Delta/\omega_m = -1$, $\alpha/\omega_m = 0.14$, $\beta/\omega_m = 0.04$, $\chi_0 = \frac{1}{2}\sqrt{\alpha^2 + \beta^2}$, $\omega_m t_0 = 40$; blue solid, the no-chirped form, $\Delta/\omega_m = 0.5$. Other parameters: $A = 0$, $B = 2 * 10^{-4}$, $\gamma/\omega_m = 10^{-5}$, $N_{th} = 50$, $\langle a(0) \rangle = 10^3$.

Fig. 2(b) of Ref. 13. There, a better cooling result is obtained with a smaller cavity damping strength. Here, we show that a smaller phonon occupation of the resonator is obtained with a larger cavity damping strength given our parameter settings. This is different from Ref. 13. This result is due to the collective effect of the cavity dissipation and the energy transfer between the cavity mode and mechanical resonator mode. By employing our chirped pulse scheme, the mechanical resonator is cooled quickly, and the phonon occupation of the resonator remains stable for relatively long time. Our proposal with a chirped pulse can be used to cool resonators efficiently in *finite time* in a large range of system parameter settings.

Methods

Applying linearization, we obtain four physical quantities δa , δb , $\langle a \rangle$, and $\langle b \rangle$ representing the operators of one cavity mode a and mechanical resonator b . To illustrate the dynamics of fluctuation components δa and δb , we use the following coupled differential equations of in rotating frame at the given driven frequency³⁶,

$$\begin{aligned} \dot{\delta a} = & \left(i\Delta + i2A\kappa\Re[\langle b(t) \rangle] - \frac{\kappa}{2} - \kappa B\Re[\langle b(t) \rangle] \right) \delta a + (iA\kappa\langle a(t) \rangle \\ & - \frac{\kappa}{2} B\langle a(t) \rangle - i\Omega(t)\frac{B}{2}) \delta b^\dagger + \left(iA\kappa\langle a(t) \rangle - \frac{\kappa}{2} B\langle a(t) \rangle \right. \\ & \left. - i\Omega(t)\frac{B}{2} \right) \delta b - \sqrt{\kappa}(1 + B\Re[\langle b(t) \rangle]) \xi_{in}, \end{aligned} \quad (7)$$

$$\begin{aligned} \dot{\delta b} = & \left(-i\omega_m - \frac{\gamma}{2} \right) \delta b + \left(iA\kappa\langle a(t) \rangle^* - i\frac{B}{2}\Omega(t)^* \right) \delta a \\ & + \left(iA\kappa\langle a(t) \rangle - i\frac{B}{2}\Omega(t) \right) \delta a^\dagger - \frac{B}{2}\sqrt{\kappa}\langle a(t) \rangle^* \xi_{in} \\ & + \frac{B}{2}\sqrt{\kappa}\langle a(t) \rangle \xi_{in}^\dagger - \sqrt{\gamma}\eta. \end{aligned} \quad (8)$$

Here, $\Delta = \omega_d - \omega_c$ is the detuning of the cavity drive, δa (δb) is the fluctuation component of the cavity mode (mechanical mode), $\langle a \rangle$ is the intra-cavity amplitude, $\Omega(t) = -i\sqrt{\kappa}\langle a_{in} \rangle$ is the amplitude of the coherent laser drive, η is the noise influencing the mechanical resonator, γ is the mechanical intrinsic damping strength, and $\Re[\langle b(t) \rangle]$ is the real part of $\langle b(t) \rangle$. The time evolution equations for $\langle a \rangle$ and $\langle b \rangle$ are

$$\begin{aligned} \langle \dot{a}(t) \rangle = & i\Delta\langle a(t) \rangle + i2A\kappa\Re[\langle b(t) \rangle]\langle a(t) \rangle - \kappa B\Re[\langle b(t) \rangle]\langle a(t) \rangle \\ & - i\Omega(t) - iB\Re[\langle b(t) \rangle]\Omega(t) - \frac{\kappa}{2}\langle a(t) \rangle, \end{aligned} \quad (9)$$

$$\begin{aligned} \langle \dot{b}(t) \rangle = & i\omega_m\langle b(t) \rangle + iA\kappa\langle a(t) \rangle^2 - \frac{\gamma}{2}\langle b(t) \rangle \\ & - i\frac{B}{2}(\Omega(t)\langle a(t) \rangle^* + \Omega(t)^*\langle a(t) \rangle). \end{aligned} \quad (10)$$

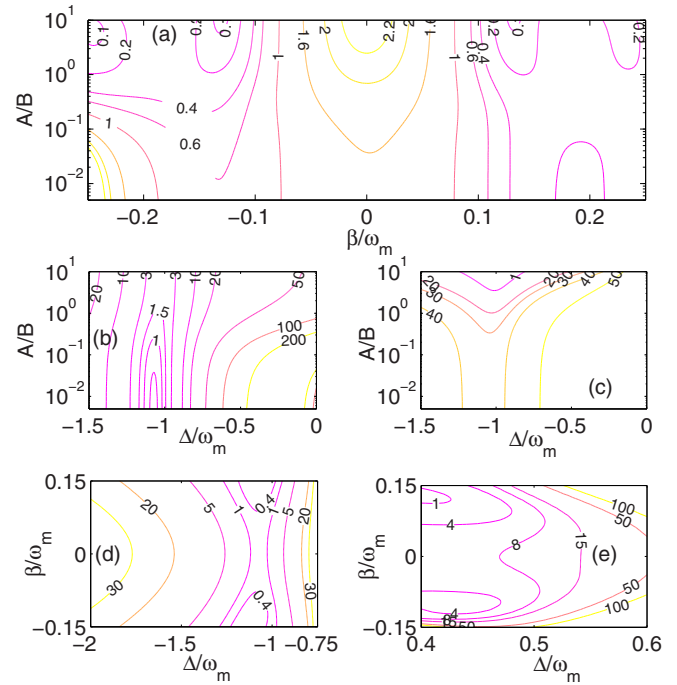


Figure 5 | The chirped pulse form, $\chi_0 = \frac{3}{2}\sqrt{\alpha^2 + \beta^2}$. (a), the effect of the optomechanical coupling strength ratio (A/B) and the strength of frequency sweeping field β/ω_m , $\alpha/\omega_m = 0.15$, $\Delta/\omega_m = -1$. (b), the effect of the optomechanical coupling strength ratio (A/B) and cavity detuning Δ/ω_m , $\alpha/\omega_m = 0.15$, $\beta/\omega_m = 0.05$. (c), a no-chirped pulse scheme, to compares with (b). (d) and (e), the strength of frequency sweeping field β/ω_m and cavity detuning Δ/ω_m to the phonon number $\langle n_{osc} \rangle = \langle \delta b^\dagger \delta b \rangle$, $A = 0$, $\alpha/\omega_m = 0.15$. For all of the plots, the time is set $\omega_m t = 70$, $B = 2 * 10^{-4}$, $\gamma/\omega_m = 10^{-6}$, $\kappa/\omega_m = 0.3$, $N_{th} = 50$, $\langle a(0) \rangle = 200$, $\omega_m t_0 = 30$.

The covariance matrix method is applied to get the phonon number of the resonator. For simplicity, we use the following expressions

$$F_1(t) = i\Delta + i2A\kappa\Re[\langle b(t) \rangle] - \frac{\kappa}{2} - \kappa B\Re[\langle b(t) \rangle], \quad (11)$$

$$F_2(t) = iA\kappa\langle a(t) \rangle - \frac{\kappa}{2} B\langle a(t) \rangle - i\frac{B}{2}\Omega(t), \quad (12)$$

$$F_3(t) = \sqrt{\kappa}(1 + B\Re[\langle b(t) \rangle]), \quad (13)$$

$$F_4(t) = iA\kappa\langle a(t) \rangle^* - i\frac{B}{2}\Omega(t)^*. \quad (14)$$

We set $\vec{V}(t) = [\delta a, \delta b, \delta a^\dagger, \delta b^\dagger]^T$, the dynamics of $\vec{V}(t)$ is satisfied by

$$\dot{\vec{V}}(t) = M(t)\vec{V}(t) + \vec{N}(t). \quad (15)$$

with

$$M(t) = \begin{pmatrix} F_1(t) & F_2(t) & 0 & F_2(t) \\ F_4(t) & -i\omega_m - \frac{\gamma}{2} & -F_4(t)^* & 0 \\ 0 & F_2(t)^* & F_1(t)^* & F_2(t)^* \\ -F_4(t) & 0 & F_4(t)^* & i\omega_m - \frac{\gamma}{2} \end{pmatrix}, \quad (16)$$

and the noise related terms,

$$\vec{N}(t) = \begin{pmatrix} -F_3(t)\xi_{in} \\ -\frac{B}{2}\sqrt{\kappa}\langle a \rangle^* \xi_{in} + \frac{B}{2}\sqrt{\kappa}\langle a \rangle \xi_{in}^\dagger - \sqrt{\gamma}\eta \\ -F_3(t)^* \xi_{in}^\dagger \\ -\frac{B}{2}\sqrt{\kappa}\langle a \rangle \xi_{in}^\dagger + \frac{B}{2}\sqrt{\kappa}\langle a \rangle^* \xi_{in} - \sqrt{\gamma}\eta^\dagger \end{pmatrix}. \quad (17)$$

We introduce a covariance matrix notation $R_{l,l'}(t) = \langle v_l(t)v_{l'}(t) \rangle$ ($l, l' = 1, 2, 3, 4$), v_l is the l th element of \vec{V} . The dynamics of R is obtained as



$$R(t) = G(t)R(0)G(t)^T + G(t)Z(t)G(t)^T, \quad (18)$$

here, $Z(t)$ is,

$$Z(t) = \int_0^t \int_0^t G(\tau)^{-1} C(\tau, \tau') [G(\tau')^{-1}]^T d\tau d\tau', \quad (19)$$

with $G(t)$ being governed by $\dot{G}(t) = M(t)G(t)$, $G(0)$ is an identity matrix, $C_{i,l}(\tau, \tau') = \langle N_l(\tau) N_l(\tau') \rangle$ ($l, l' = 1, 2, 3, 4$), N_l is the l th element of \vec{N} . By considering a Markovian bath, we write $C(\tau, \tau')$ as $C(\tau)\delta(\tau - \tau')$, and the matrix expression of $C(\tau)$

$$C(\tau) = \begin{pmatrix} 0 & -F_3(\tau) \frac{\beta}{2} \sqrt{\kappa} \langle a(\tau) \rangle & |F_3(\tau)|^2 & F_3(\tau) \frac{\beta}{2} \sqrt{\kappa} \langle a(\tau) \rangle \\ 0 & -\frac{\beta}{4} \kappa |\langle a(\tau) \rangle|^2 & \frac{\beta}{2} \sqrt{\kappa} F_3(\tau)^* \langle a(\tau) \rangle^* & \frac{\beta}{4} \kappa |\langle a(\tau) \rangle|^2 + \gamma(N_{th} + 1) \\ 0 & 0 & 0 & 0 \\ 0 & \frac{\beta}{4} \sqrt{\kappa} |\langle a(\tau) \rangle|^2 + \gamma N_{th} & -\frac{\beta}{2} \sqrt{\kappa} F_3(\tau) \langle a(\tau) \rangle^* & -\frac{\beta}{4} \kappa |\langle a(\tau) \rangle|^2 \end{pmatrix}. \quad (20)$$

Here, N_{th} is the distribution of the thermal bath surrounding the mechanical resonator.

- Clerk, A. A., Devoret, M. H., Girvin, S. M., Marquardt, F. & Schoelkopf, R. J. Introduction to quantum noise, measurement, and amplification. *Rev. Mod. Phys.* **82**, 1155–1208 (2010).
- Aspelmeyer, M., Kippenberg, T. J. & Marquardt, F. Cavity Optomechanics. *arXiv:1303.0733v1*. (a review on cavity optomechanics, <http://arxiv.org/abs/1303.0733>).
- Law, C. K. Interaction between a moving mirror and radiation pressure: A Hamiltonian formulation. *Phys. Rev. A* **51**, 2537 (1995).
- Marquardt, F., Chen, J. P., Clerk, A. A. & Girvin, S. M. Quantum Theory of Cavity-Assisted Sideband Cooling of Mechanical Motion. *Phys. Rev. Lett.* **99**, 093902 (2007).
- Wilson-Rae, I., Nooshi, N., Zwerger, W. & Kippenberg, T. J. Theory of Ground State Cooling of a Mechanical Oscillator Using Dynamical Backaction. *Phys. Rev. Lett.* **99**, 093901 (2007).
- Wilson-Rae, I., Nooshi, N., Dobrindt, J., Kippenberg, T. J. & Zwerger, W. Cavity-assisted backaction cooling of mechanical resonators. *New. J. Phys.* **10**, 095007 (2008).
- Genes, C., Vitali, D., Tombesi, P., Gigan, S. & Aspelmeyer, M. Ground-state cooling of a micromechanical oscillator Comparing cold damping and cavity-assisted cooling schemes. *Phys. Rev. A* **77**, 033804 (2008).
- Tian, L. Cavity cooling of a mechanical resonator in the presence of a two-level-system defect. *Phys. Rev. B* **84**, 035417 (2011).
- Wang, X., Vinjanampathy, S., Strauch, F. W. & Jacobs, K. Ultraefficient Cooling of Resonators: Beating Sideband Cooling with Quantum Control. *Phys. Rev. Lett.* **107**, 177204 (2011).
- Machnes, S. *et al.* Pulsed Laser Cooling for Cavity Optomechanical Resonators. *Phys. Rev. Lett.* **108**, 153601 (2012).
- Allen, L. & Eberly, J. H. *Optical resonance and two-level atoms* (Dover, New York, 1987).
- Hioe, F. T. Solution of Bloch equations involving amplitude and frequency modulations. *Phys. Rev. A* **30**, 2100 (1984).
- Liao, J. Q. & Law, C. K. Cooling of a mirror in cavity optomechanics with a chirped pulse. *Phys. Rev. A* **84**, 053838 (2011).
- Gu, W. J. & Li, G. X. Quantum interference effects on ground-state optomechanical cooling. *Phys. Rev. A* **87**, 025804 (2013).
- Liu, Y. C., Xiao, Y. F., Luan, X. & Wong, C. W. Dynamic Dissipative Cooling of a Mechanical Resonator in Strong Coupling Optomechanics. *Phys. Rev. Lett.* **110**, 153606 (2013).
- Liu, Y. C., Hu, Y. W., Wong, C. W. & Xiao, Y. F. Review of cavity optomechanical cooling. *Chin. Phys. B* **22**, 114213 (2013).
- Arcizet, O., Cohadon, P. F., Briant, T., Pinard, M. & Heidmann, A. Radiation-pressure cooling and optomechanical instability of a micromirror. *Nature* **444**, 71 (2006).
- Gigan, S. *et al.* Self-cooling of a micromirror by radiation pressure. *Nature* **444**, 67 (2006).
- Schliesser, A., Rivière, R., Anetsberger, G., Arcizet, O. & Kippenberg, T. J. Resolved-sideband cooling of a micromechanical oscillator. *Nat. Phys.* **4**, 415 (2008).
- Gröblacher, S. *et al.* Demonstration of an ultracold micro-optomechanical oscillator in a cryogenic cavity. *Nat. Phys.* **5**, 485 (2009).

- Schliesser, A., Arcizet, O., Rivière, R., Anetsberger, G. & Kippenberg, T. J. Resolved-sideband cooling and position measurement of a micromechanical oscillator close to the Heisenberg uncertainty limit. *Nat. Phys.* **5**, 509 (2009).
- Park, Y. S. & Wang, H. Resolved-sideband and cryogenic cooling of an optomechanical resonator. *Nat. Phys.* **5**, 489 (2009).
- Rivière, R. *et al.* Optomechanical sideband cooling of a micromechanical oscillator close to the quantum ground state. *Phys. Rev. A* **83**, 063835 (2011).
- Chan, J. *et al.* Laser cooling of a nanomechanical oscillator into its quantum ground state. *Nature* **478**, 89 (2011).
- Teufel, J. D. *et al.* Sideband cooling of micromechanical motion to the quantum ground state. *Nature* **475**, 359 (2011).
- Verhagen, E., Deléglise, S., Weis, S., Schliesser, A. & Kippenberg, T. J. Quantum-coherent coupling of a mechanical oscillator to an optical cavity mode. *Nature* **482**, 63 (2012).
- Regal, C. A., Teufel, J. D. & Lehnert, K. W. Measuring nanomechanical motion with a microwave cavity interferometer. *Nat. Phys.* **4**, 555 (2008).
- Teufel, J. D., Harlow, J. W., Regal, C. A. & Lehnert, K. W. Dynamical Backaction of Microwave Fields on a Nanomechanical Oscillator. *Phys. Rev. Lett.* **101**, 197203 (2008).
- Li, M., Pernice, W. H. P. & Tang, H. X. Tunable bipolar optical interactions between guided lightwaves. *Nat. Photon.* **3**, 464 (2009).
- Xuereb, A., Schnabel, R. & Hammerer, K. Dissipative Optomechanics in a Michelson-Sagnac Interferometer. *Phys. Rev. Lett.* **107**, 213604 (2011).
- Yan, M. Y., Li, H. K., Liu, Y. C., Jin, W. L. & Xiao, Y. F. Dissipative optomechanical coupling between a single-wall carbon nanotube and a high-Q microcavity. *Phys. Rev. A* **88**, 023802 (2013).
- Sawadsky, A. *et al.* Observation of generalized optomechanical coupling and cooling on cavity resonance. *arXiv:1409.3398v1*. (an observation of dispersive and dissipative couplings, <http://arxiv.org/abs/1409.3398>).
- Elste, F., Girvin, S. M. & Clerk, A. A. Quantum Noise Interference and Backaction Cooling in Cavity Nanomechanics. *Phys. Rev. Lett.* **102**, 207209 (2009).
- Elste, F., Girvin, S. M. & Clerk, A. A. Erratum: Quantum Noise Interference and Backaction Cooling in Cavity Nanomechanics. *Phys. Rev. Lett.* **103**, 149902 (2009).
- Weiss, T. & Nunnenkamp, A. Quantum limit of laser cooling in dispersively and dissipatively coupled optomechanical systems. *Phys. Rev. A* **88**, 023850 (2013).
- Weiss, T., Bruder, C. & Nunnenkamp, A. Strong-coupling effects in dissipatively coupled optomechanical systems. *New. J. Phys.* **15**, 045017 (2013).
- Li, M., Pernice, W. H. P. & Tang, H. X. Reactive Cavity Optical Force on Microdisk-Coupled Nanomechanical BeamWaveguides. *Phys. Rev. Lett.* **103**, 223901 (2009).
- Walls, D. F. & Milburn, G. J. *Quantum optics* (Springer, Berlin, 1994).

Acknowledgments

We are grateful to Prof. L.C. Kwek for reading and revising the manuscript. We acknowledge the financial support in part by the 10000-Plan of Shandong province, and the National High-Tech Program of China grant No. 2011AA010800 and 2011AA010803, NSFC grant No. 11474182, 11174177 and 60725416.

Author contributions

T.C. and X.W. contributed equally to this work.

Additional information

Competing financial interests: The authors declare no competing financial interests.

How to cite this article: Chen, T. & Wang, X.-B. Fast cooling in dispersively and dissipatively coupled optomechanics. *Sci. Rep.* **5**, 7745; DOI:10.1038/srep07745 (2015).



This work is licensed under a Creative Commons Attribution-NonCommercial-NoDerivs 4.0 International License. The images or other third party material in this article are included in the article's Creative Commons license, unless indicated otherwise in the credit line; if the material is not included under the Creative Commons license, users will need to obtain permission from the license holder in order to reproduce the material. To view a copy of this license, visit <http://creativecommons.org/licenses/by-nc-nd/4.0/>